PAPER Nr. : 58

EXPERIENCE WITH A NEW APPROACH TO ROTOR AEROELASTICITY

BY

M.H. PATEL and G.T.S. DONE

The City University,
London, U.K.

TENTH EUROPEAN ROTORCRAFT FORUM

AUGUST 28 – 31, 1984 – THE HAGUE, THE NETHERLANDS

EXPERIENCE WITH A NEW APPROACH TO ROTOR AEROELASTICITY

by

M.H. Patel and G.T.S. Done
The City University, London, U.K.

Abstract

Experience with an alternative procedure for computing the aeroelastic stability of a helicopter rotor system is described. The method has already been presented at a previous European Rotorcraft Forum, and is aimed at generating the coefficients of the aeroelastic equations of motion automatically on the computer. The main objective of the current work is to validate the associated computer program using three practical examples provided by Westland Helicopters Ltd. These examples are graded such that different aspects of the program are tested. The validation exercise is completed by comparing the results obtained by the new method with those previously obtained using conventional techniques, and providing explanation for discrepancies where they occur.

1. Introduction

A technique for obtaining the matrix coefficients of the aeroelastic equations of motion of a helicopter rotor system which saves time by avoiding the need for extensive algebraic derivation and manipulation has been described, and the philosophy and general method outlined, by Gibbons and Done.[1] It relies on a computer program which contains, in effect, a description of the mathematical model of the system through the transformation matrices that identify in space any material point on the helicopter, and which, in addition to integrations, performs numerically all differentiations including those required in the Lagrange equations formulation. In Ref. 1, expressions are given for the matrix coefficients of the aeroelastic equations of motion; these are integrals (over a surface or a volume) of the dot product of two (3 x 1) vectors, the components of which are themselves partial differentials of various order with respect to generalised co-ordinates and/or time. These are reproduced for convenience in Appendix A.1. Then, once the form of the transformations required to express the displacement of a point in blade axes in terms of space fixed axes has been defined, as in Appendix A.2, the integrations required can be simplified in nature, depending on the coefficient type involved. A very simple example of a rigid blade having flap, lag and pitch freedoms was studied in Ref. 1, primarily to test the accuracy that would be expected from the various orders of numerical differentiation formulae. The equations of motion themselves are implied from the computed coefficients and apply to perturbation co-ordinates linearised about an equilibrium state.

This approach appears quite similar to that of Lytwyn,[2] but contrasts with that of Nagabhushanam et al[3] which uses a symbolic processor for algebraic manipulation to obtain the equations of motion in explicit and fully non-linear form directly from the computer.

It is probably fair to say that none of these computer based methods is intended particularly to lead to an increased understanding of the various factors that are important in helicopter aeroelasticity. This can be gained by study of the wealth of previously published work, comprehensively reviewed by Friedmann.[4,5] However, any technique which reduces the time spent in designing an aeroelastically satisfactory rotor system is of interest to industry, and thus it was that a series of validation exercises was drawn up, so that industry would feel confident in using the computer program on new rotor designs.

A significant advantage of the current approach is that no ordinary procedure for dealing with small order terms is necessary. All terms, large or small, are inherently maintained in what is effectively the computer's formulation. This is particularly advantageous with the newer forms of rotor system in which the amount of coupling present between separate blade motions may be relatively large.

The three verification exercises are based on three distinct problems, all previously analysed conventionally by Westland Helicopters Ltd. (WHL). These are conveniently described as:

(a) Sea King tail rotor
(b) Lynx rotating blade
(c) Lynx ground resonance.

These cases test various aspects of the computer program, as indicated in Table 1.1.

Table 1.1: Aspects of the computer program tested by cases (a), (b) and (c)

Aspect	Case		
	(a)	(b)	(c)
Strip theory aerodynamics	✓		✓
Steady-state solution	✓		
Blade coupling effects (apart from δ_3 and α_2)		✓	
Non-fixed rotor axis			✓
Gravity terms			✓
Blade flexural modes		✓	✓
Blade twist/pitch modes		✓	

In each case, the computer program was arranged to follow as closely as possible the analysis procedure previously adopted by WHL; i.e. the initial data, the order of the various transformations and the general mathematical modelling were maintained. The results are presented in the following Sections and the reasons for discrepancies where they occur, are provided.

2. First verification exercise - Sea King tail rotor

The Sea King tail rotor model comprises a rigid blade rotating about a fixed axis and having three degrees of freedom, flap, lag and pitch. The axes of these freedoms pass through the rotation axis.

The results apply for the case of zero blade section c.g. offset, rotation speed Ω = 132.2 rad/s and steady-state values of β_0 = 0.0881 rad (flap up), ζ_0 = -0.0206 rad (backward lag) and Θ_0^0 = 0.436 rad (applied pitch nose up). These steady-state values were obtained using the program in which the structural stiffnesses are as provided by WHL and with a pitch-flap mechanical coupling of $\delta_3 = 45^0$. The original WHL values were 0.0871 rad and -0.0203 rad for flap and lag respectively.

The verification exercise consisted of producing the mass-dependent and aerodynamic coefficient matrices for the given steady-state condition, comparing with the previous Westland results, and examining and explaining discrepancies. It is not considered relevant in a paper of this nature to reproduce all the matrices which were computed. Instead, only those which highlight the reasons for discrepancies are shown. The first of these is the mass-dependent stiffness matrix (centrifugal effects) which is shown below in Table 2.1 for two cases, the suffices i = 1, 2 applying as follows:

1 - computer program results
2 - Westland results as provided.

Table 2.1: Mass-dependent stiffness matrices

($\underset{\sim}{R}$ is a stiffness matrix, and suffix 'm' refers to mass contribution.)

$$\underset{\sim}{R}_{m1} = 10^3 \begin{bmatrix} 377.5 & 1.071 & -0.6446 \\ 1.071 & -3.183 & -0.0525 \\ -0.6446 & -0.0525 & 0.594 \end{bmatrix}$$

$$\underset{\sim}{R}_{m2} = 10^3 \begin{bmatrix} 381.7 & -0.3054 & -0.6519 \\ -0.3054 & 0 & -0.0529 \\ -0.6519 & -0.0529 & 0.601 \end{bmatrix}$$

The 12 term shows a significant discrepancy. This was found to be due to the omission of an apparently second order small term from the WHL analysis. This extra term is:

$$\Omega^2 I_0 \zeta_0 (-\beta_0 \cos\beta_0 - \sin\beta_0 + \zeta_0^2 \sin\beta_0 \cos\beta_0 + \tfrac{1}{2}\beta_0^2 \sin\beta_0) \quad .. (2.1)$$

where I_0 is the blade flapping inertia. When introduced, the result becomes 1.069×10^3 which agrees with the computer program result. For the 22 term, there is a similar omitted term which is:

$$\Omega^2 I_0 (-1 + \cos\beta_0 - \tfrac{1}{2}\beta_0^2 \cos\beta_0 - \tfrac{3}{2}\zeta_0^2 \cos^2\beta_0)$$

giving a value of -3.198×10^3, which agrees reasonably well with the program result in $\underset{\sim}{R}_{m1}$.

The fact that the direct lag stiffness term is negative is due to the lagging transformation following after the flap transformation, leading to lagging effectively taking place in a plane tilted at the flap angle, rather than in a cone. The tendency is for the blade to lag back to a zero flap angle position, thus providing a destabilising effect. Reversing the order of the flap and lag transformations would lead to different coefficients.

The aerodynamic damping and stiffness matrices were computed, and again it is in the stiffness terms that the more noticeable discrepancies occur. The matrices are shown below in Table 2.2.

Table 2.2: Aerodynamic stiffness matrices

(Suffix 'a' refers to aerodynamic contribution.)

$$\underset{\sim}{R}_{a1} = 10^4 \begin{bmatrix} 15.73 & 1.382 & -15.74 \\ -3.426 & 0.0252 & 3.279 \\ 0 & 0 & 0 \end{bmatrix}$$

$$\underset{\sim}{R}_{a2} = 10^4 \begin{bmatrix} 16.112 & 1.2771 & -15.823 \\ -3.258 & -0.2721 & 3.194 \\ 0 & 0 & 0 \end{bmatrix}$$

The reason for the discrepancy in the 22 term was found to be due to the omission of one of the transformations in the Westland analysis, so that the aerodynamic forces were not quite resolved correctly, the effect being most noticeable in this term. Other differences are due to the fact that no approximations are made for trigonometric functions of small angles in the computer program.

The discrepancies found in all the matrices are not significant in practical terms; an eigenvalue analysis of the resultant equations derived by the two techniques showed negligible difference.

3. Second verification exercise - Lynx rotating blade

This exercise concerns only the natural frequencies and normal mode shapes of a Lynx blade, rotating about a fixed axis. Aerodynamic forces are excluded. The objective was to provide the program with the set of six frequencies and mode shapes previously computed by Westland as input information, and test if the data were correctly returned on output.

The original results for the blade had been computed using a transfer matrix method based on over 900 spanwise points along the blade axis. The modal data were then interpolated to provide results (deflections, slopes and curvatures) at 25 evenly spaced points. The mass, inertia and stiffness distributions were provided at their original unevenly spaced data points, as well as at the 25 interpolated points. The sectional inertias and stiffnesses were given in flatwise and edgewise directions. In addition, torsional stiffness and pitch control stiffness and geometry were provided.

In the event, it transpired that the discrepancies that arose were largely due to the fact that the interpolated results provided by WHL already embodied a small but significant loss of accuracy due to the numerical process of reducing the data by interpolation. Much effort went into trying to minimise this drawback. Because it was considered that using the physical data points (i.e. points where there are significant mass or stiffness changes) for the computer program integration points (rather than the arbitrary equi-spaced points), the modal deflections and slopes are interpolated back on to 30 selected physical data points. The very rapid changes of stiffness along the blade (see Fig. 1) make straight-forward interpolation unsuitable for curvatures, so the results in this case are obtained by interpolating the product of flexural rigidity (EI) and curvature, and subsequently dividing by the local EI.

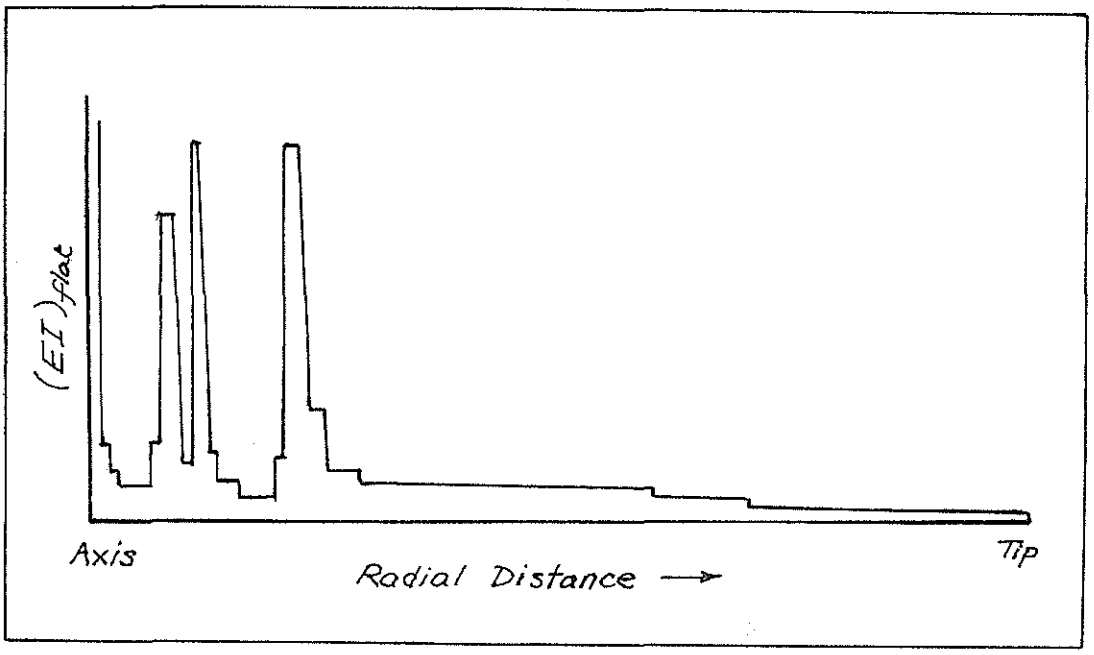

Fig. 1: Flatwise flexural rigidity variation along blade span

The geometry of the blade pitch control is shown in Fig. 2 and is such that flap and pitch are coupled. However, it may be seen that there is a bending moment discontinuity at the connection of the pitch control horn with the blade, and thus the interpolation for curvatures is not carried across this point. This is important in computing structural stiffness contributions involving flatwise bending. The blade rate of twist (leading to torsional stiffness contributions) is discontinuous here anyway, since the pitch feathering bearing separates the blade structure at this point.

The blade axis is offset from a radial axis and is pre-coned; additionally the blade has built-in twist and the sectional centre of mass is variably offset from the blade axis. Collective pitch is applied so that the nominal blade pitch runs from 18^{o} inboard to 12^{o} nose up at the tip. The rotation speed is 34.17 rad/s.

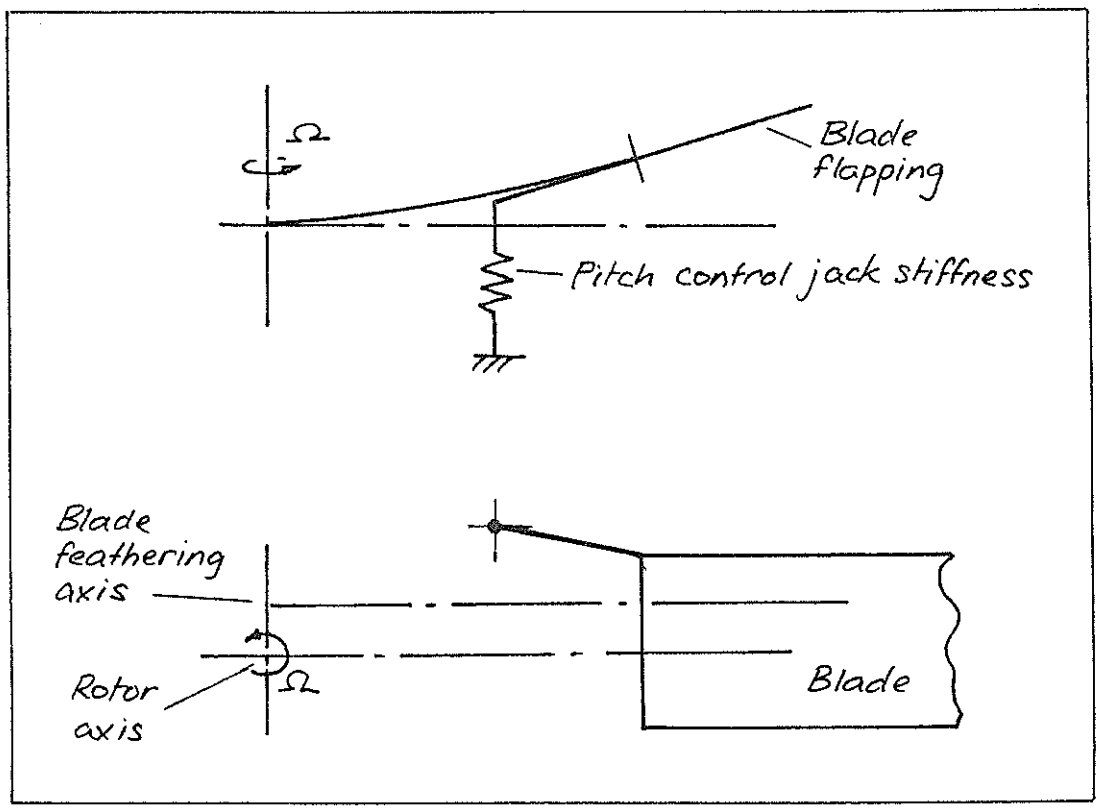

Fig. 2: Blade pitch control geometry

The results for the six eigenvalues, or rotating natural frequencies, are compared in Table 3.1.

Table 3.1: Natural frequencies (based on blade rotation speed Ω = 34.17 rad/s)

Mode	Approximate description	Frequency (per rotor revolution)	
		Westland	Program
1	1st lag	0.647	0.647
2	1st flap	1.109	1.107
3	2nd flap	2.690	2.701
4	1st pitch/twist	3.875	3.911
5	2nd lag	4.296	4.292
6	3rd flap	4.939	4.984

Also shown, in Table 3.2, is the modal matrix returned by the computer program. A column in this matrix indicates the proportion of the original six mode shapes present in a computed mode shape.

Ideally, if there were no loss of accuracy, this matrix would be the unit matrix. The deviation from unity indicates the loss of accuracy.

Table 3.2: Modal matrix

0.999	0.004	0.007	0.001	-0.023	0
-0.003	1	-0.022	0.021	-0.002	-0.025
-0.002	0.002	0.999	0.087	0.009	-0.016
0	0	-0.004	0.987	0.007	0.004
0	0	-0.009	-0.054	0.999	-0.056
0.001	0	0.004	-0.012	0.042	0.998

Considering the loss of accuracy that is inherent in the previously mentioned interpolation of input data, the results in Tables 3.1 and 3.2 are within acceptable bounds. It may be observed, however, that the fourth mode which is mainly blade pitch and twist is the least easy to reproduce. The reason for this is that the contributions to the kinetic and potential energies from flap and lag, despite the fact that geometrically the role of these motions is small, remain dominant so that any inaccuracies that are present tend to increase the apparent couplings between this mode and adjacent modes.

The mode shapes are shown in Figs. 3 to 8. Each Figure provides the variation of flap and lag displacement radially and also the variation of local pitch angle. Flapping up, lagging forwards and pitching nose up are taken as positive. Where a component of the overall deformation is insignificant, it is shown multiplied by 10 in a Figure, so that a sensible comparison between the computer program results and the initial mode shape data may be made. The results compare well on the whole with the least good reproduction occurring for the pitch/twist contribution of the mainly second lag and third flap modes of Figs. 7 and 8.

The effect previously noted in this Section of the initial interpolation of input data was confirmed by carrying out the exercise described for both 25 and 30 integration points, based on selected physical data points. For 25 points, the mean of the moduli of all the off-diagonal terms in the modal matrix is 0.034; for 30 points (i.e. for the matrix shown in Table 3.2), this figure decreased to 0.014.

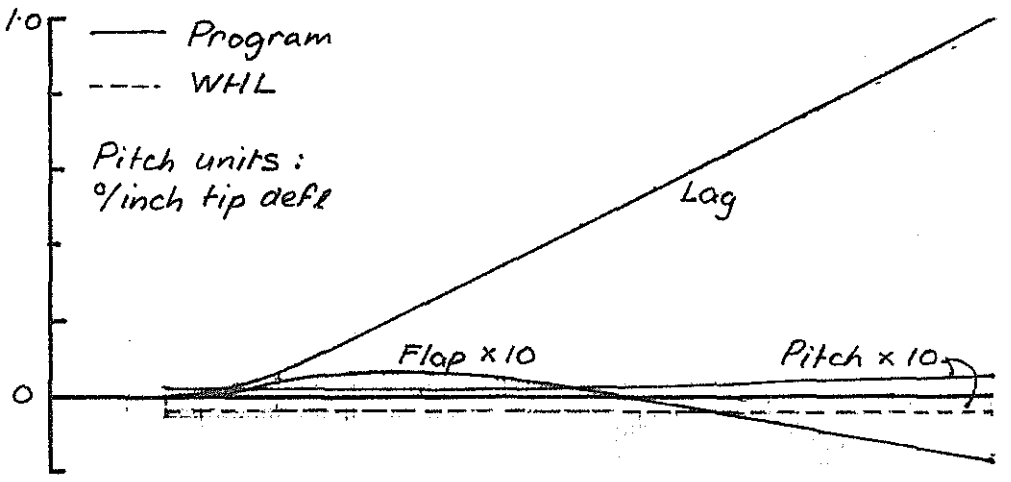

Fig. 3: Fundamental lag mode

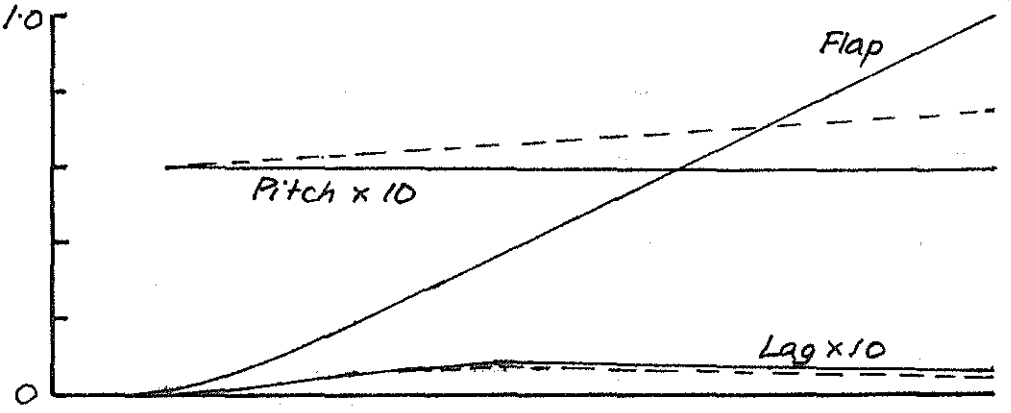

Fig. 4: Fundamental flap mode

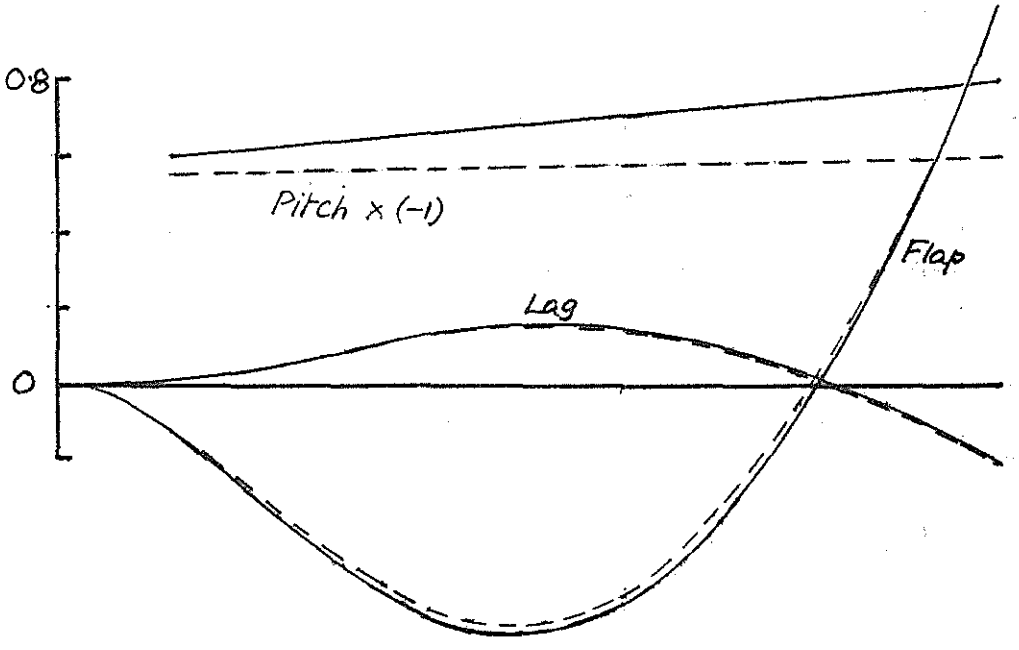

Fig. 5: Second flap mode

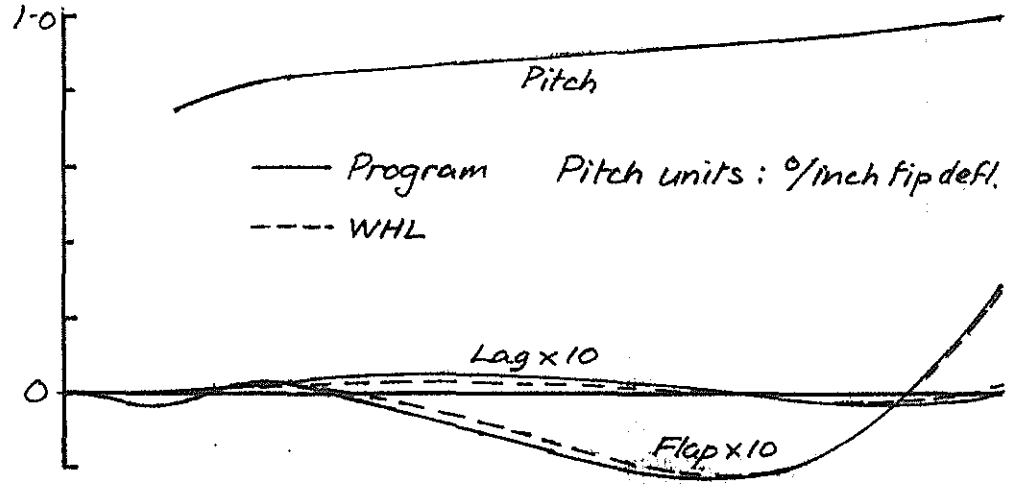

Fig. 6: Fundamental pitch/twist mode

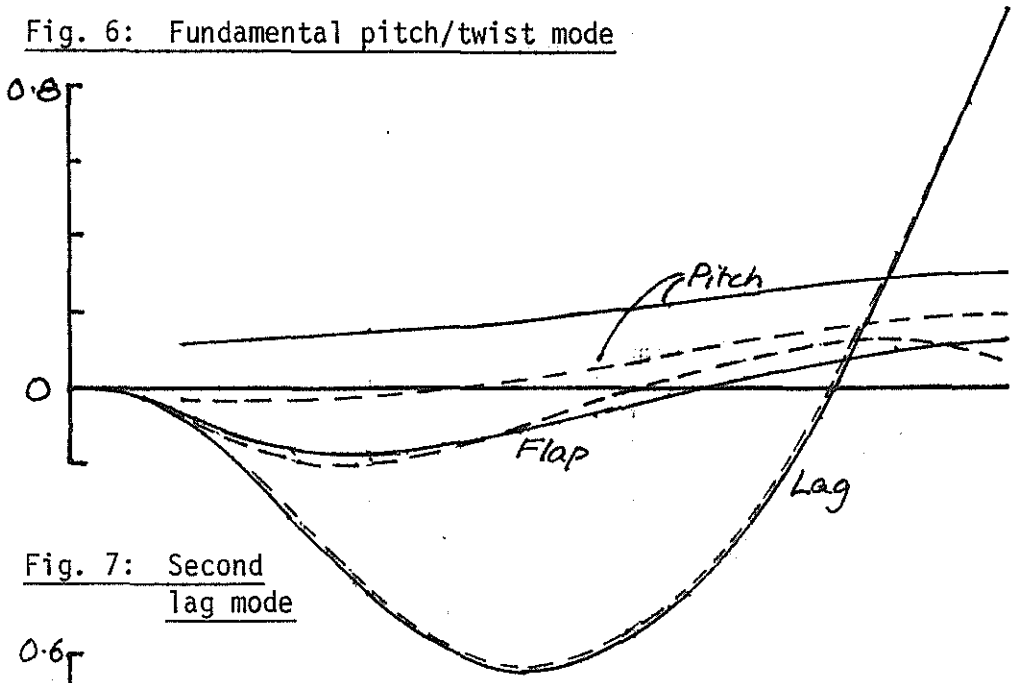

Fig. 7: Second lag mode

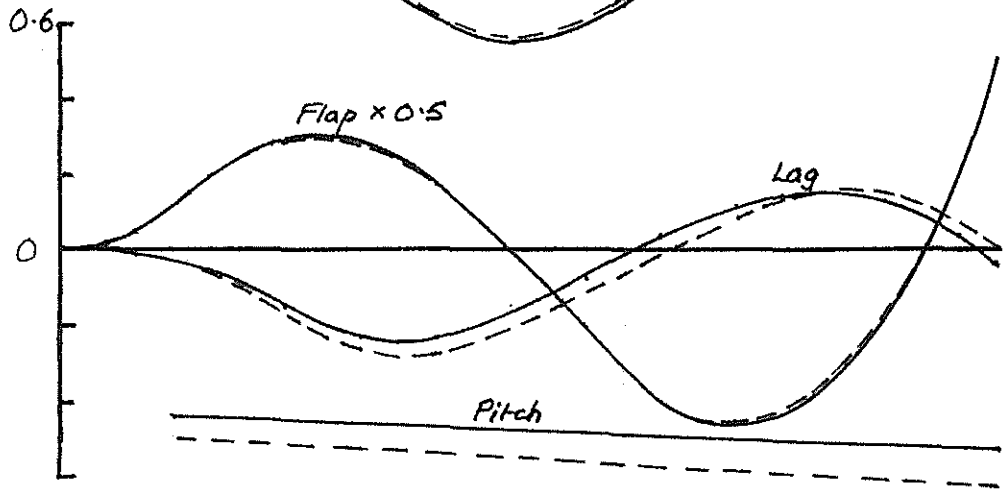

Fig. 8: Third flap mode

4. Third verification exercise - Lynx ground resonance

This exercise is aimed at determining the validity of the program when fuselage and undercarriage effects are incorporated. The major difference between this exercise and the previous two is that the rotor axis is not fixed; because of the fuselage freedoms it is able to rotate and translate. The computer program is used to produce coefficient matrices at a particular time instant, and a Coleman transformation applied to provide a set of constant coefficient matrices. The eigenvalues of the associated equations of motion are then computed for a particular rotor angular speed.

The fuselage is assumed to be a rigid body having five degrees of freedom, made up of the three translation freedoms and two rotations (roll and pitch). Yaw is excluded.

The fuselage-undercarriage effects are based on the actual test results in which the rotor system had been replaced by an equivalent mass at the hub. The mode shapes yielded by the tests are used to determine the fuselage damping and stiffness terms. The drive shaft is tilted forwards relative to the aircraft vertical axis and two degrees of freedom, a pure flap and a pure lag with previously determined mode shapes, are allowed for each of the four main rotor blades giving 13 dof's in all. In order to conform to the WHL analysis, the blade mass is assumed to be concentrated along a single curve. As such an assumption is equivalent to setting the sectional edgewise and lagwise radii of gyration and the c.g. offsets to be zero, the differentials of many matrices for the mass contributions are not required, thereby reducing the computation time. This time was further reduced by limiting the number of integration points to 25 over the radius.

The results for the eigenvalues, at a rotor angular speed of 34.17 rad/s, are shown in Table 4.1.

Table 4.1: Real and imaginary parts of eigenvalues, ground resonance problem

Previous WHL results		Computer program results	
Real	Imaginary	Real	Imaginary
-2.401	0	-2.40	0
-0.329	1.043	-0.310	1.031
0.0014	1.911	0.0019	1.919
-0.1788	2.19	-0.176	2.184
-0.0251	3.519	-0.0230	3.514
-0.0252	3.522	-0.0231	3.515
-2.523	5.457	-2.52	5.42
-2.521	5.458	-2.53	5.43
-0.0193	9.335	-0.0183	9.33
-2.517	10.901	-2.521	10.87
-1.203	23.97	-1.203	23.97
-1.276	25.468	-1.271	25.41
-1.432	27.65	-1.435	27.65

It may be seen that there are no significant differences between the two sets of results.

Because the eigenvalues provide only an overall indication of the degree of verification provided, a detailed comparison of the coefficient matrices at the particular time instant t = 0 (i.e. before applying the Coleman transformation) has also been conducted. The mode numbering system in the tables of results is as follows in Table 4.2.

Table 4.2: Mode numbering system

Mode No.	Component	Description
1	Fuselage	Fore & aft translation
2	"	Sideways translation
3	"	Heave
4	"	Roll
5	"	Pitch
6	Blade 1	Flap
7	" 2	"
8	" 3	"
9	" 4	"
10	Blade 1	Lag
11	" 2	"
12	" 3	"
13	" 4	"

At the time instant taken, blade 1 is pointing forwards, blade 2 to port, 3 backwards and blade 4 to starboard.

As an example of how the comparison of matrix coefficients was conducted, separate contributions of part of the stiffness matrix are shown in Tables 4.3 and 4.4. The first Table shows the mass contribution (i.e. centrifugal effects) and the second shows the contribution from aerodynamic forces. The total stiffness matrix is given by summing these two contributions with the structural stiffness (no contribution in the particular sub-matrix represented by the Tables) and the gravitational stiffness terms.

Numbers appear in pairs in the Tables, the upper coming from the computer program and the lower from the previous WHL computations. Similar results for zero blade pre-cone and zero rotor axis tilt were obtained, thereby allowing explanations for noticeable differences in pairs of numbers to be found. For example, the 3-6 and 3-8 terms in Table 4.3 (at the time instant under consideration, fore and aft pointing blades flapping coupling with fuselage heave) in the latter case are zero, identifying the reason for the discrepancies as being due to lack of second order rotor tilt effects in the WHL analysis. In Table 4.4 there are significant discrepancies in the 4-11 and 4-13 terms, and the 5-10 and 5-12 terms (sideways pointing blades lagging coupling with fuselage roll, and fore and aft pointing blades lagging coupling with fuselage pitch, respectively). The coupling terms for the individual blade aerodynamic flapping stiffness due to lag (terms

Table 4.3: Mass contributions to stiffness sub-matrix

		Blade Flap				Blade Lag			
	Mode No.	6	7	8	9	10	11	12	13
Fuselage Freedoms	1	1398 1371		-1398 -1371			33678 33610		-33678 -33610
	2		1400 1371		-1400 -1371	-33740 -33610		33740 33610	
	3	-85.1 0		85.1 0			-2050 -2043		2050 2043
	4		512610 510530	0.018 -0.166	-512610 -510530	147930 146640		-147930 -146640	0 -0.277
	5	-513580 -510590	0 -59.3	513580 510470	0 -58.1		147740 146640		-147740 -146640

Table 4.4: Aerodynamic contributions to stiffness sub-matrix

		Blade Flap				Blade Lag			
	Mode No.	6	7	8	9	10	11	12	13
Fuselage Freedoms	1	1782 1809	17.52 13.26	-1763 -1800	0.91 -4.51	-138.9 -148.8	82.6 98.0	276.0 314.5	54.8 65.0
	2	-8.32 -8.88	1776 1806	8.32 8.88	-1776 -1805	-13.9 -15.0	-208.1 -231.7	13.9 15.0	208.1 231.7
	3	43.4 47.0	150.9 156.0	259.3 267.0	151.8 157.0	1142 1364	1128 1353	1116 1344	1130 1356
	4	-1831 -1837	-5398 -5460	1805 1819	5372 5440	-21125 -21210	19335 23222	21002 21190	-19458 -23247
	5	5405 5550	-1786 -1811	-5335 -5430	1856 1845	-19170 -22920	-20842 -20890	19690 23548	21340 21510

6-10, 7-11, etc., not shown in Table 4.4) are similar in magnitude and difference, being 17460 and 20,950 respectively. All these terms disappear for zero blade pre-cone and rotor tilt, which implies inappropriate treatment of small order steady-state angles in the WHL analysis, rather similar to that for the Sea King tail rotor example in Section 2. In order to keep these numbers in perspective, it should be noted that the overall direct stiffness coefficients associated with the degrees of freedom involved above are of magnitude 10^6.

The rest of the stiffness matrix, the damping matrix (containing aerodynamic, mass and structural contributions) and inertia matrix exhibited no significant differences requiring explanation.

5. Discussions and conclusions

The main conclusion from the three verification exercises described in the foregoing Section was that confidence had been established in the computer program, and the outcome is that the program is now mounted and running at WHL, Yeovil. As an example of the computing time taken, the complete set of matrices for the Lynx ground resonance case took 2½ minutes to produce on the Westland computer, compared with 1 s to produce the same matrices conventionally from analytic expressions.

The main difficulties encountered were in interpreting the models presented in exactly the same manner they had been interpreted by Westland, in ensuring that the large volume of data had been correctly transcribed, and in dealing with data which was, in effect, only an imperfect subset of the original data (as in the case of the Lynx rotating blade example). It should be observed that these difficulties arise as a result of performing a verification exercise, and are not inherent in the method itself.

The advantage of not requiring to define an ordering scheme is well highlighted by the first and third examples when the method is compared with a derivation based on a paper analysis, in which an ordering scheme is necessary to minimise the workload on the analyst. Another advantage, of course, is that the overall time taken from model definition to final result is much shorter. The main disadvantage is that insight and "feel" for important parameters are lost. Furthermore, changes to one or two parameters would, at present, involve re-running the whole, or major parts of the program. Although only simple aerodynamic modelling was used in the present examples, more complicated models which cannot be easily expressed analytically may be accommodated without too much extra difficulty. For the test cases considered a linearised analysis is adequate, but it is felt that the current technique may hold significant advantages when applied to future systems.

When comparing the present method with one based on algebraic or symbolic computing (as in Ref. 3), the situation is somewhat different. In this case, an ordering procedure is not strictly necessary, although, if it is absent, the computing time could be considerable and the equations produced in algebraic form would be too involved for sensible inspection as they stand. Substitution of the data into the equations leads to numbers which are no more or less informative than the numbers provided by the current approach. However, changes in parameters (the basic model remaining effectively the same) can be more happily countenanced. Until the same model, or a very similar model, is treated by both methods, though, it will remain difficult to form precise comparisons.

The current programme of verification concerns axial flow situations. Future work will cover forward flight and improved models for various aspects such as aerodynamics and blade pitch control.

6. Acknowledgements

The authors would like to express their appreciation to Dr. S.P. King and Mr. P.T.W. Juggins of Westland Helicopters Ltd., and to Mr. A.J. Sobey of the R.A.E., Farnborough, for their continued support and encouragement. This work is funded by the Ministry of Defence.

7. References

(1) M.P. Gibbons and G.T.S. Done, Automatic Generation of Helicopter Rotor Aeroelastic Equations of Motion, Proc. 8th European Rotorcraft Forum, Aix-en-Provence, Paper No. 3.3, Aug/Sept, 1982.

(2) R.T. Lytwyn, Aeroelastic Stability Analysis of Hingeless Rotor Helicopters in Forward Flight Using Blade and Airframe Normal Modes, Proc. 36th Annual National Forum of AHS, Paper No. 24, May, 1980.

(3) J. Nagabhushanam, G.H. Gaonkar and T.S.R. Reddy, Automatic Generation of Equations of Rotor-body Systems with Dynamic Inflow for a Priori Ordering Scheme, Proc. 7th European Rotorcraft Forum, Garmisch-Partenkirchen, Paper No. 37, Sept., 1981.

(4) P.P. Friedmann, Recent Developments in Rotary-wing Aeroelasticity, J.Aircraft, 14, 11, Nov, 1977.

(5) P.P. Friedmann, Formulation and Solution of Rotary-wing Aeroelastic Stability and Response Problems, Vertica, 7, 2, 1983.

Appendix A.1: Expressions for matrix coefficients

The full derivation for the expressions which appear below is given in Ref. 1. The coefficients are the elements of the matrices [P], [Q] and [R] in the equations of motion:

$$[P]\ddot{\underset{\sim}{q}} + [Q]\dot{\underset{\sim}{q}} + [R]\underset{\sim}{q} = \underset{\sim}{0} \qquad .. \text{(A.1.1)}$$

in which $\underset{\sim}{q}$ is a vector of generalised co-ordinates representing perturbations from some steady-state situation. The matrix coefficients are:

$$P_{ij} = \int \frac{\partial \underset{\sim}{R}}{\partial q_i} \cdot \frac{\partial \underset{\sim}{R}}{\partial q_j} \, dm \qquad .. \text{(A.1.2)}$$

$$Q_{ij} = 2\int \frac{\partial \underset{\sim}{R}}{\partial q_i} \cdot \frac{\partial^2 \underset{\sim}{R}}{\partial q_j \partial t} \, dm - \int \frac{\partial \underset{\sim}{R}}{\partial q_i} \cdot \frac{\partial \underset{\sim}{F}}{\partial q_j} \, dS \qquad .. \text{(A.1.3)}$$

$$R_{ij} = \int \frac{\partial \underset{\sim}{R}}{\partial q_i} \cdot \frac{\partial^3 \underset{\sim}{R}}{\partial q_j \partial t^2}\, dm - \int \frac{\partial^2 \underset{\sim}{R}}{\partial q_i \partial q_j} \cdot \frac{\partial^2 \underset{\sim}{R}}{\partial t^2}\, dm \qquad .. (A.1.4)$$

$$- \int \frac{\partial \underset{\sim}{R}}{\partial q_i} \cdot \frac{\partial \underset{\sim}{F}}{\partial q_j}\, dS - \int \frac{\partial^2 \underset{\sim}{R}}{\partial q_i \partial q_j} \cdot \underset{\sim}{F}\, dS$$

$$- \int \frac{\partial^2 U}{\partial q_i \partial q_j}\, dV$$

in which $\underset{\sim}{R}$ is the position vector of a point in the helicopter with reference to space fixed or inertial axes, $\underset{\sim}{F}$ is the aerodynamic force vector per unit area referred to the same axes, U is strain energy, dm is an elemental mass, dS an elemental area and dV an elemental volume. The integral signs are symbolic, the integration being as indicated by dm, dS or dV and over an appropriate extent, e.g. the total number of blades, the blade lifting surface, the fuselage, etc. The dot products ensure that the integrals are of scalar quantities. Structural damping is introduced into [Q] separately.

To evaluate the integrals, $\underset{\sim}{R}$ and $\underset{\sim}{F}$ have to be expressed in terms of local co-ordinates by means of a set of transformations (see Appendix A.2); the differentials are performed numerically for a given time instant and the integrations (also numerical) are arranged so that, for a blade, they utilise blade properties expressed along a blade axis. The general scheme is explained in Ref. 1.

Appendix A.2: Formulation of transformation from local to fixed axes

Figs. 9(a) and (b) show the various deformations and axes that enable the transformation from local co-ordinates based on moving axes to co-ordinates based on fixed or inertial axes to be made. The flap, lag and twist deformations are expressed in terms of assumed modes, each of these being associated with a generalised co-ordinate, q_i. The assumed modes may be experimentally obtained or previously calculated, or based on some simple algebraic form, e.g. polynomial, trigonometric etc. Thus:

$$\left.\begin{aligned} f_\beta(s) &= \beta_o s + f_{\beta o}(s) + \sum_i f_{\beta i}(s) q_i \\ f\zeta(s) &= \zeta_o s + f_{\zeta o}(s) + \sum_i f_{\zeta i}(s) q_i \\ \Theta_s(s) &= \Theta_o(s) + \Theta_{os}(s) + \sum_i f_{\theta i}(s) q_i \end{aligned}\right\} \qquad .. \qquad .. (A.2.1)$$

in which $f_\beta(s)$, $f_\zeta(s)$ and $\Theta_s(s)$ are the flap, lag and pitch deflections at a station distance s along the blade axis, β_o is the coning angle, ζ_o the steady lag, and Θ_o the combined built-in twist

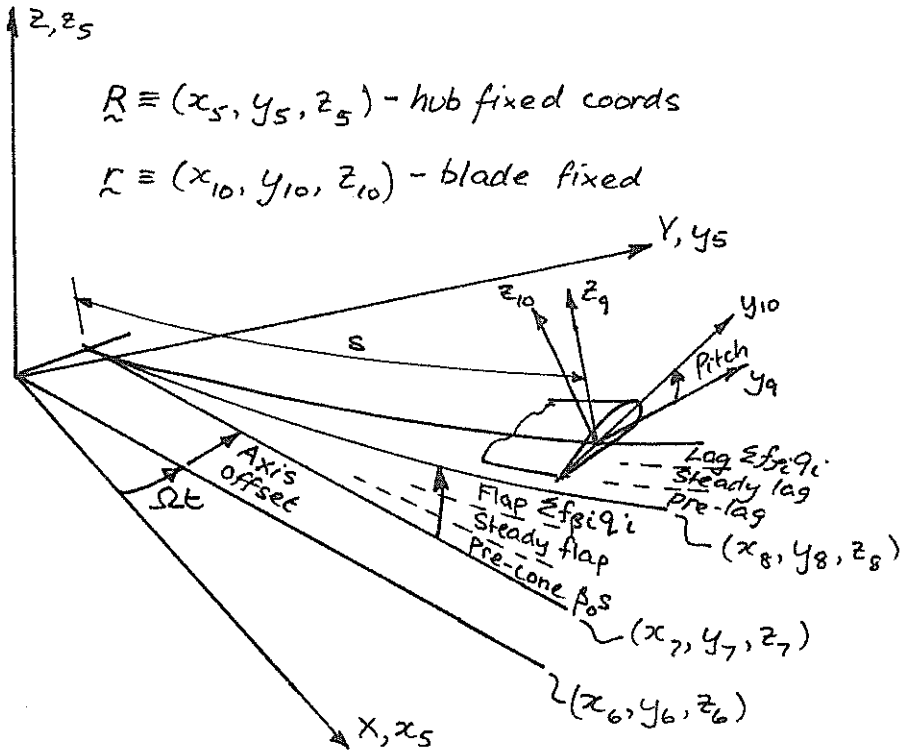

Fig. 9(a): Transformations to hub-fixed axes

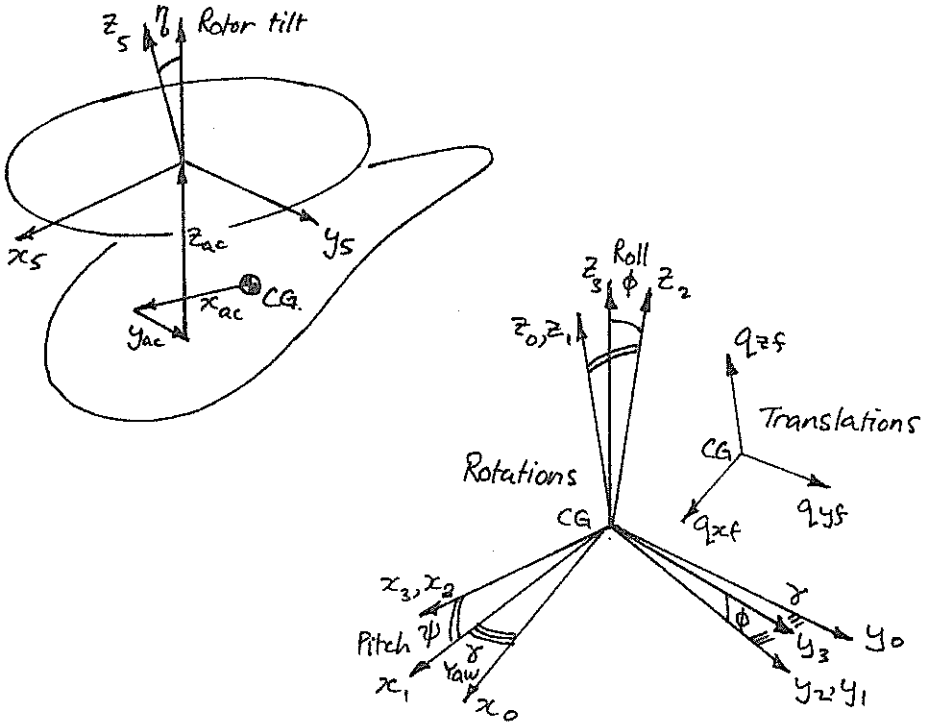

Fig. 9(b): Transformations to space-fixed axes

and applied pitch. The sectional steady-state values are given by $f_{\beta o}(s)$, $f_{\zeta o}(s)$ and $\Theta_{os}(s)$, and the contributions from each mode q_i are $f_{\beta i}(s)$, $f_{\zeta i}(s)$ and $f_{\theta i}(s)$. Any mechanical pitch/flap or pitch/lag coupling terms (i.e. due to δ_3 and α_2) would appear in the expression for $\Theta_s(s)$. Differentiation of $f_\beta(s)$ and $f_\zeta(s)$ with respect to s provides expressions for local flap and lag angles, $\beta(s)$ and $\zeta(s)$ respectively. Further angles, necessary to formulate rotation transformation matrices are $T \equiv \Omega t$ (instantaneous angle of rotation of the datum blade about the rotor axis), η (rotor axis tilt), and ϕ, ψ, γ (fuselage roll, pitch and yaw).

It can be shown that a point at $\underset{\sim}{r}_{10} \equiv \{x_{10}, y_{10}, z_{10}\}$ on a blade (local blade axes with $x_{10} = 0$, see Fig. 9(a)) may be expressed in terms of axes attached to the rotor hub as

$$\underset{\sim}{r}_h \equiv \{x_5, y_5, z_5\}$$

$$= [A_1]\underset{\sim}{r}_{10} + \underset{\sim}{B}_1 \qquad .. \qquad .. \qquad .. \qquad .. \quad (A.2.2)$$

where $[A_1] = [T_T][T_\beta][T_\zeta][T_\theta]$

$$[B_1] = [T_T](\underset{\sim}{r}_6 + [T_\beta]\underset{\sim}{r}_5)$$

$$\underset{\sim}{r}_5 = \begin{bmatrix} -\frac{1}{2}\int_0^s \zeta(s)^2 ds \\ f_\zeta(s) \\ 0 \end{bmatrix}$$

$$\underset{\sim}{r}_6 = \begin{bmatrix} s - \frac{1}{2}\int_0^s \beta(s)^2 ds \\ Y_o \\ Z_o + f_\beta(s) \end{bmatrix}$$

in which Y_o and Z_o define the built-in blade axis offset. A rotational transformation matrix is denoted $[T_{(angle)}]$; the angle indicates the angle between the axes concerned. A typical matrix is, for example:

$$[T_\theta] = \begin{bmatrix} 1 & 0 & 0 \\ 0 & \cos\Theta(s) & -\sin\Theta(s) \\ 0 & \sin\Theta(s) & \cos\Theta(s) \end{bmatrix}$$

The diagonal positioning of the 'one' depends upon the axes about which the rotational transformation is taking place.

For axes fixed in space:

$$\underset{\sim}{r}_o \equiv \{x_o, y_o, z_o\}$$

$$= [A]\underset{\sim}{r}_{1o} + \underset{\sim}{B} \quad .. \quad .. \quad .. \quad .. \quad \text{(A.2.3)}$$

where $[A] = [T_\gamma][T_\psi][T_\phi][T_\eta][A_1]$

$$\underset{\sim}{B} = [T_\gamma][T_\psi][T_\phi]([T_\eta]\underset{\sim}{B}_1 + \underset{\sim}{r}_{ac}) + \underset{\sim}{r}_f$$

in which $\underset{\sim}{r}_{ac}$ defines the co-ordinates of the aircraft centre of mass, and $\underset{\sim}{r}_f \equiv \{q_{xf}, q_{yf}, q_{zf}\}$ is a vector of the fuselage translational displacements (see Fig. 9(b)).